Experimental Gerontology 45 (2010) 457–463

Contents lists available at ScienceDirect

Experimental Gerontology

journal homepage: www.elsevier.com/locate/expgero

Decrease in PTEN and increase in Akt expression and neuron size in aged rat spinal cord

Miguel Augusto Rodrigues de Amorim [a], Luis Miguel Garcia-Segura [a,*], Rodolfo Gustavo Goya [b], Enrique Leo Portiansky [c]

[a] Instituto Cajal, CSIC, E-28002 Madrid, Spain
[b] INIBIOLP-Histology B, School of Medicine, National University of La Plata, 1900 La Plata, Argentina
[c] Institute of Pathology, School of Veterinary Sciences, National University of La Plata, 1900 La Plata, Argentina

ARTICLE INFO

Article history:
Received 7 January 2010
Received in revised form 18 March 2010
Accepted 19 March 2010
Available online 27 March 2010

Keywords:
Aging
Morphometry
Motoneurons
Neuronal size
Protein phosphatase

ABSTRACT

PTEN is a tumor suppressor gene known to play an important role in the regulation of cell size. In this study we compared PTEN expression in the spinal cord of young (5 months old) vs. aged (32 months old) female rats and correlated them with alterations in neuron size and morphology in the same animals. Total and phosphorylated PTEN (pPTEN) as well as its downstream target phosphorylated Akt (pAkt) were assessed by Western blotting. Spinal cord neurons were morphometrically characterized. Total PTEN, pPTEN and total Akt expression were significantly higher in young rats than in aged animals. Expression of pAkt was stronger in aged animals. A significant increase in neuronal size was observed in large motoneurons of aged as compared with young rats. Our data show that in the spinal cord of rats, neuronal PTEN expression diminishes with advanced age while neuronal size increases. These results suggest that in the spinal cord, an age-related reduction in PTEN and increase of pAkt expression may be involved in the progressive enlargement of neurons.

1. Introduction

The impact of aging on the spinal cord has received significantly less attention than in other central nervous system structures. In previous studies we have detected age associated changes in lectin affinity (Lozza et al., 2009), as well as in the expression of intermediate filaments (Fontana et al., 2009) and in the neuronal marker NeuN (Portiansky et al., 2006) in the spinal cord of female rats.

PTEN (phosphatase and tensin homologue on chromosome 10) is a tumor suppressor gene that can inhibit cell growth, proliferation and migration and that controls apoptosis in a number of cell types, mainly through inhibition of the phosphoinositide 3-kinase (PI3K) signaling pathway (Fraser et al., 2004; Kwon et al., 2006; van Diepen and Eickholt, 2008). PTEN gene product has lipid phosphatase activity against the 3′phosphate group of phosphatidylinositol 3,4,5 trisphosphate. PI3K catalyzes the inverse reaction, resulting in serine/threonine-specific protein kinase (Akt) activation. Abnormalities in many components of the PI3K/Akt pathway have been associated with diverse brain disorders such as tumors, schizophrenia and autism (Kwon et al., 2006) and Lhermitte-Duclos disease (Backman et al., 2001; Kwon et al., 2001).

PTEN is expressed during neurite extension, and PTEN expression is essential for survival of differentiating neuronal cells (Stiles et al., 2004). It may inhibit cell migration, spreading, and focal adhesion formation by dephosphorylating the focal adhesion kinase (Ross et al., 2001). The PI3K/Akt pathway has also been linked to activity-dependent plasticity processes in the brain. It has been shown that PTEN negatively controls proliferation of neural stem cells and that is required for normal migration of postmitotic neurons (Groszer et al., 2001; Otaegi et al., 2006).

The aim of the present study was to assess the impact of aging on total PTEN, phosphorylated PTEN (pPTEN), total Akt and phosphorylated Akt (pAkt) levels in the spinal cord of rats. Since PTEN plays an important role in the regulation of cell size (Kwon et al., 2001; Stiles et al., 2004; Yue et al., 2005), we compared the above mentioned biochemical age changes with those in spinal neuron size.

2. Methods

2.1. Animals

Young (5 months old) and aged (32 months old), clinically healthy Sprague Dawley female rats were used. Range body weight of the animals was 180–200 g (young) and 230–240 g (aged). Animals were anaesthetized with an i.m. injection of ketamine

* Corresponding author. Address: Instituto Cajal, CSIC, Avenida Doctor Arce 37, E-28002 Madrid, Spain. Tel.: +34 915854729; fax: +34 915854754.
E-mail address: lmgs@cajal.csic.es (L.M. Garcia-Segura).

0531-5565/$ - see front matter © 2010 Elsevier Inc. All rights reserved.
doi:10.1016/j.exger.2010.03.015

hydrochloride (40 mg/kg) followed by an i.m. injection of xylazine (Rompun®, Bayer; 8 mg/kg). Rats used for Western blot analysis were sacrificed by decapitation. All other rats were perfused through the left ventricle with 4% para-formaldehyde solution in PBS 0.1 M, pH 7.4 during 30 min. Animals were sacrificed following the international rules specified at "Guidelines on the Use of Animals in Neuroscience Research (The Society of Neuroscience)" and "Research Laboratory Design Policy and Guidelines of NIH".

2.2. Western blotting and antibodies

For Western blotting processing, spinal cords of decapitated rats were immediately frozen until use. The entire spinal cord (young $n = 4$; aged $n = 3$) was homogenized in lysis buffer containing 150 mM NaCl, 20 mM Tris, pH 7.4, 10% glycerol, 1 mM EDTA, 1% NP40 (Roche, Mannheim, Germany) supplemented with protease and phosphatase inhibitors (50 μg/ml phenylmethylsulfonyl fluoride, 10 μg/ml aprotinin, 25 μg/ml leupeptin and 100 nM orthovanadate, all from Sigma–Aldrich Corp., St. Louis, MO).

Homogenates were allowed to solubilize for 15 min on ice and centrifuged at 21,900*g* for 15 min at 4 °C. Protein content of the supernatant was measured with a modified Bradford assay (BioRad Laboratories, Munich, Germany). Proteins (30 μg) were resolved by sodium dodecylsulphate–polyacrylamide gel electrophoresis (SDS–PAGE) in a Mini-Protein system (BioRad) and transferred to nitrocellulose membranes. The membranes were blocked with 5% non-fat milk diluted in TTBS (20 mM Tris–HCl, pH 7.5, 500 mM NaCl, 0.05% Tween 20) and incubated overnight at 4 °C with the primary antibodies. The following antibodies were used: anti-total PTEN (mouse monoclonal, Santa Cruz Biotechnology, Santa Cruz, CA; diluted, 1:1000); anti-phosphorylated ser380PTEN (rabbit polyclonal, Cell Signaling Technology diluted, 1:1000); antiAkt1/2 (rabbit polyclonal, Santa Cruz Biotechnology; diluted 1:2000); anti-phosphorylated-Akt Ser473 (rabbit polyclonal, Cell Signaling Technology; diluted 1:1000); and anti-GADPH/glyceraldehyde-3-phosphate dehydrogenase (mouse monoclonal, Millipore/Chemicon; diluted 1:3000). After incubation with the primary antibody, the membranes were washed and incubated for 2 h at room temperature with an anti-mouse or anti-rabbit antibody coupled to horseradish peroxidase (Jackson ImmunoResearch Europe, Newmarket, Suffolk, UK; diluted 1:10,000), to recognize the corresponding primary antibodies. Immunoreactive bands were detected using an enhanced chemiluminescence system (ECL, Amersham Pharmacia Biotech, Piscataway, NJ), followed by apposition of the membranes to autoradiographic films. Films were analyzed using the Molecular Dynamics Image Quant software version 3.22 (Computing densitometer model 300A, Molecular Dynamics, Buckinghamshire, UK). The density of each band was normalized to GADPH acting as a loading control. In order to minimize inter-assay variations, samples from all animal groups, in each experiment, were processed in parallel.

2.3. Immunohistochemistry

The spinal cord of 3 young and 3 aged rats was removed from the spine, equilibrated in a cryoprotecting solution containing 30% sucrose, 0.1 M PB (0.1 M Na_2HPO_4 buffer) in H_2O and stored at −20 °C until processing. Segments C1, C5, C8, T8 and L3 were prepared for vibratome sectioning. Twenty-micrometer coronal sections of every segment were sectioned (VT 1000 S, Leica Microsystems, Wetzlar, Germany) and mounted on gelatin coated slides for staining with cresyl violet.

Immunohistochemistry was carried out in free-floating sections (40 μm coronal sections of every segment) under moderate shaking. The endogenous peroxidase activity was quenched for 10 min at room temperature in a solution of 3% hydrogen peroxide in 30% methanol. After several washes in 0.1 M phosphate buffer pH 7.4, containing 0.3% bovine serum albumin, 0.3% Triton X-100, and 0.9% NaCl (washing buffer), sections were incubated for 48 h at 4 °C with a mouse monoclonal antibody for total PTEN (Santa Cruz; diluted, 1:600). Primary antibodies were diluted in washing buffer containing 3% normal goat serum. After incubation with the primary antibody, sections were then rinsed in buffer and incubated for 2 h at room temperature with biotinylated goat anti-mouse (Pierce, Rockford, IL; diluted 1:300 in washing buffer). After several washes in buffer, sections were incubated for 90 min at room temperature with avidinbiotin–peroxidase complex (ImmunoPure ABC peroxidase staining kit, Pierce; diluted 1:300). The reaction product was revealed by incubating the sections with 0.05% 3,3′-diaminobenzidine (Sigma–Aldrich) and 0.01% hydrogen peroxide in 0.1 M phosphate buffer. Counterstaining was performed using Mayer's haematoxylin. Negative controls, omitting the primary antibodies were also evaluated.

2.4. Immunofluorescence

A similar protocol was followed for simultaneous immunofluorescent localization of PTEN and phosphorylated-ser380PTEN (pPTEN). For this purpose monoclonal antibody for total PTEN (Santa Cruz; diluted, 1:1000) or rabbit polyclonal antibody for pPTEN (Santa Cruz; diluted 1:2000) were used. Goat anti-mouse or anti-rabbit IgG conjugated with Alexa488 or Alexa555 (Molecular Probes, Madrid, Spain; diluted 1:1000), for PTEN or pPTEN, respectively, was used as secondary antibody. Controls omitting either primary antibody against PTEN or pPTEN were included to insure that double label signals did not reflect artifactual crosstalk. Nuclei were stained with DAPI. Sections were observed and images were obtained in an Olympus BX61 microscope.

2.5. Morphometry

Morphometry on neuronal cells was carried out on digital images obtained from vibratome sectioned cresyl violet stained slides. Images were captured through a camera (DP71, Olympus, Tokyo) attached to a microscope (Olympus BX61, Japan) and processed using an image analysis software (ImagePro Plus, v6.3, Media Cybernetics, USA). Raw images (RGB 24 bits TIFF format) obtained from 5 non-contiguous sections of every cervical segment, cut 100 μm apart were used for determination of the integrated optical density (IOD) of the stained structures. IOD was obtained by multiplying the cell area by its mean optical density. For doing so, images of the entire spinal cord section were tiled using a motorized stage (H101 CNL1, Prior, USA). All images were captured in the same session with the same parameters of magnification, intensity of light, condenser aperture and setting of microscopic filters. After capturing of the images, background correction was performed in all of them. In order to select the positively stained area (peroxidase staining) for further IOD determination, and to separate it from the counterstained or not stained tissues the "color segmentation process" was applied. A mask was then applied to make the separation of colors permanent. Images where then converted to an 8-bit gray-scale TIFF format. After intensity of light calibration of images, the IOD of each labeled neuron was obtained.

Data obtained was exported to a spreadsheet in order to perform statistical analysis. All images were subjected to blind routine analysis by an experienced morphologist.

In order to determine the morphometric characteristics of neuronal bodies, segmentation based on staining color was performed. Segment C8 was used as a model for morphometric determination. Neurons were then characterized using the following parameters: cellular area (area of each object), major and minor cell diameter

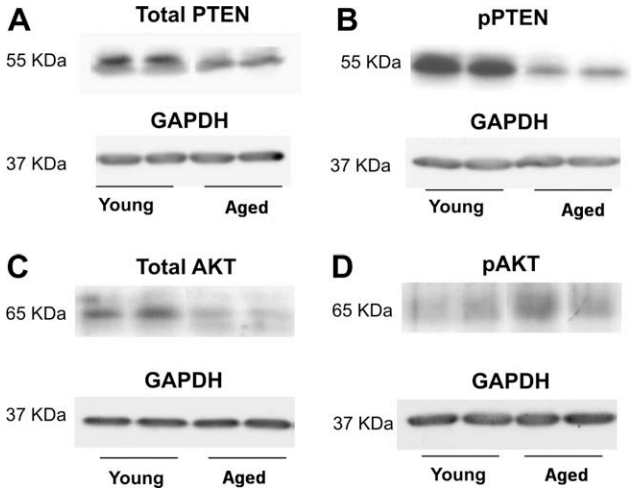

Fig. 1. Western blots analysis. Samples obtained from the spinal cord of young and aged rats for total PTEN (A), pPTEN (B), total Akt (C) and pAkt (D) are presented. GAPDH was used as loading control. Both bands shown in panel A were densitometrically analyzed.

(length of the longest and shortest lines, respectively, joining two outline points and passing through the centroid), perimeter (length of the outline of each object) and roundness (circle-likeness of each object). The fact that cresyl violet does not stain glial cell somas, stains differentially glial and neuronal nuclei and considering glial nuclei diameter is below 7 μm, allowed us to safely eliminate (manually and automatically) glial cells during cell recognition.

Morphometric data were taken only from those neuronal somas that showed a delineated shape and a distinguishable nucleus. Similarly, only those cells that were recognized by the image analyzer, based on the staining or color pattern and on their size and shape, were included in the analysis.

Neuronal bodies of every segment lamina (Lm-I to Lm-X) were classified in groups (according to their major diameter length) as small (5–10 μm), medium (10–15 μm) and large (larger than 15 μm) as suggested by Rexed (1952). However, since the embedding process produces an isotropic contraction of the tissue (Schüz and Palm, 1989), ranges were increased in 40% (i.e., 7–14 μm, 14–21 μm, more than 21 μm for small, medium and large neurons, respectively).

2.6. Colocalization analysis

Colocalization analysis of PTEN and pPTEN labeling was performed in images of the spinal cord segments. Briefly, monochrome images were pseudocolored using the dye list function of the image analysis program. For quantifying the colocalization indexes of both labels, the Colocalization function of the analysis image program was used and the Mander overlap coefficient (Zinchuk and Zinchuk, 2006) (*R*) calculated (value 0.0 for no colocalization; 1.0 for 100% colocalization of two intensity patterns (Agnati et al., 2005)). The overlap coefficients k1 and k2 were used to determine the contribution of each antigen to the areas with colocalization (values are variable).

2.7. Statistics

Morphometric data was analyzed with a mixed model for repeated measures (Littell et al., 1998). Fixed effects included in the model were age of the rat (young, aged), cell size (small, medium, large), and lamina (Lm-I to Lm-X), as well as the triple interaction between the three effects. Animal was a random effect, and the covariance structure of the error terms included an autoregressive of order one block structure within animal across laminas. Estimable functions involving the parameters due to age and terms of the interaction age * size * lamina were used to test whether there were differences between young and aged rats for each combination of cell size and lamina. *P* values <0.05 were considered to indicate significant differences.

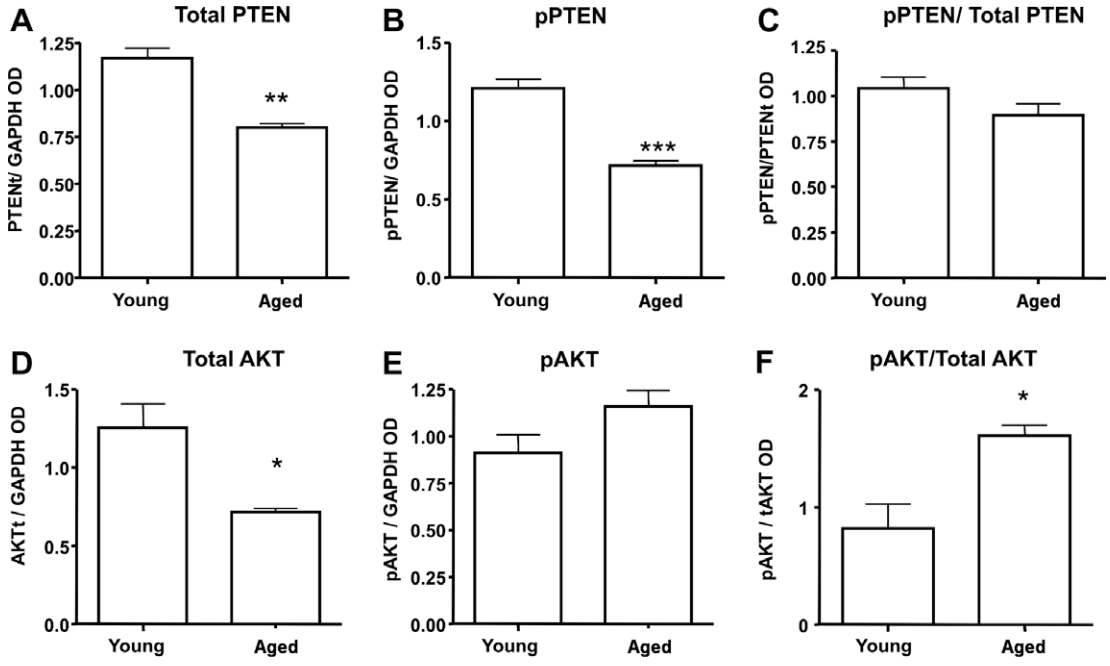

Fig. 2. Densitometric analysis of the Western blot. Graphs represent bands for total PTEN (A), pPTEN (B) and the ratio between both of them (C). The same analysis was performed for total Akt (D), pAkt (E) and their ratio (F). Data were normalized to GAPDH values and expressed as means ± SEM. * Significant differences ($P < 0.05$) vs. the values of the young animals. ** $P < 0.01$; *** $P < 0.001$.

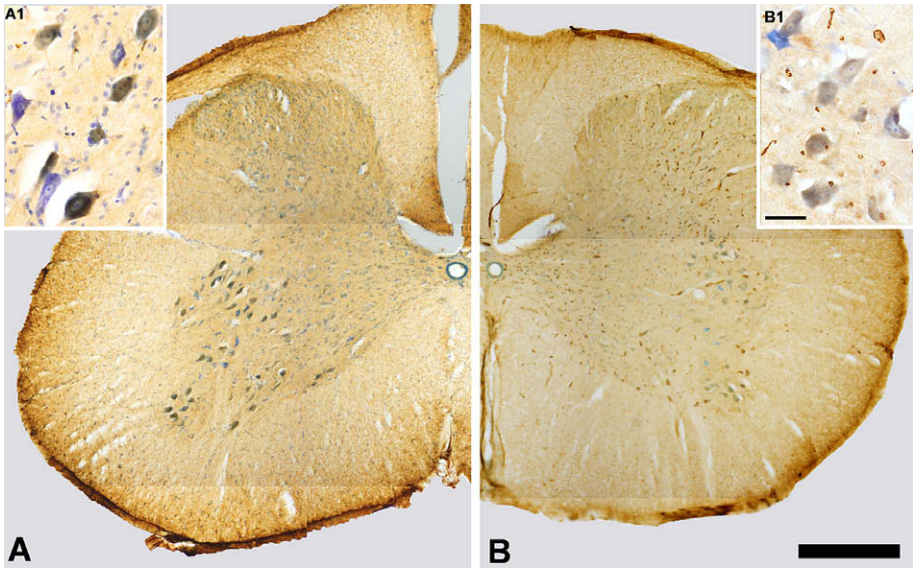

Fig. 3. Expression of PTEN in the cervical spinal cord segments of young and aged rats. Cervical segments from young and aged rats were incubated with mouse mAb against total PTEN as described in Materials and methods. Not all of the segments showed the same staining pattern. Panels A and B show the hemisections of C8 of young (A) and aged (B) female rats. As can be seen, the labeling intensity was stronger in A. Even though the apparent distribution was located in Lm-IX, the other laminas were stained although less intensely. The marker was mainly located in the cytoplasm but was also observed inside the nuclei. Insets A1 and B1 are magnifications of their respective samples. Bar = 0.5 mm. Bar for insets = 50 μm.

IOD data obtained was statistically assessed by the Anova test. The Bonferroni method was used as a post hoc test. *P* values <0.05 were considered to indicate significant differences.

3. Results

3.1. Effect of aging on biochemical expression of markers

Western blots from total and pPTEN in the spinal cord (Fig. 1A and B) showed a double band pattern in both age groups at the expected molecular weight of 55 kDa. However, the double band had a different profile in young and aged rats. In young rats the weaker band was located below the stronger one, while the opposite occurred in the aged animals. This may be due to different forms of the PTEN protein that are recognized by the total-PTEN antibody. It is possible, that the upper band represents a phosphorylated form of PTEN, since the upper band in the blot for total PTEN behaves in the same fashion as that of pPTEN.

Fig. 1C and D show Western blots obtained for Akt and phosphorylated Akt (pAkt). The results of the densitometry analysis of the bands are shown in Fig. 2. The expression of total PTEN was significantly higher in young than in aged animals (young:aged ratio 1.5:1). Moreover, the same pattern was observed for pPTEN. Since both isoforms of PTEN behaved in the same fashion, no statistical differences were observed when calculating their ratio (Fig. 2A).

The expression of total Akt was significantly higher in young rats when compared with aged animals (young:aged ratio 1.5:1). This pattern was inverted when analyzing pAkt expression which was stronger in aged animals (young:aged ratio 0.75:1). The pAkt:-total Akt ratio was significantly different in both age groups (Fig. 2B).

3.2. Effect of aging on immunohistochemical expression of markers

All the histological sections from young rats, except for some of the C5 segment, showed, when assessed visually, a stronger immunoreactivity for total-PTEN antibody compared to aged tissues (Fig. 3). Staining was mainly localized at the Lm-IX (motoneurons), but was also seen in the remaining laminas (Lm-I, Lm-VII, Lm-X) albeit with much less intensity. The cellular pattern of immunoreactivity was mainly cytoplasmic although nuclear staining was also observed (Fig. 3, insets A and B). In all cases, only neurons were stained. IOD morphometry revealed that even though visual observation of the slides suggested a difference between ages, statistical significance was only observed at C8 (Fig. 4).

3.3. Immunofluorescence studies

Double immunofluorescence labeling with PTEN and pPTEN revealed that both proteins showed over an 85% colocalization. Both proteins showed a granular pattern distributed in the entire neuroplasm (Fig. 5A–F). The overlap colocalization coefficient k2 related to pPTEN was always greater than k1 (related to PTEN) (range k1:k2 0.75:1) being significant for T8 and L3 in young animals. In all cases, k1 value increased with age but not significantly. The opposite was true for k2 except for C5.

3.4. Impact of aging on spinal cord neuron size

Morphometric analysis of each lamina in C8 segments revealed that in both young and aged animals the mean value of the area of

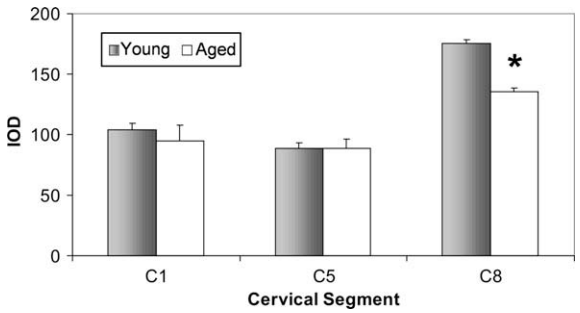

Fig. 4. Integrated Optical Density (IOD) of the labeling against PTEN. A significant age-related difference was observed in the IOD of segment C8 but not in C1 and C5.

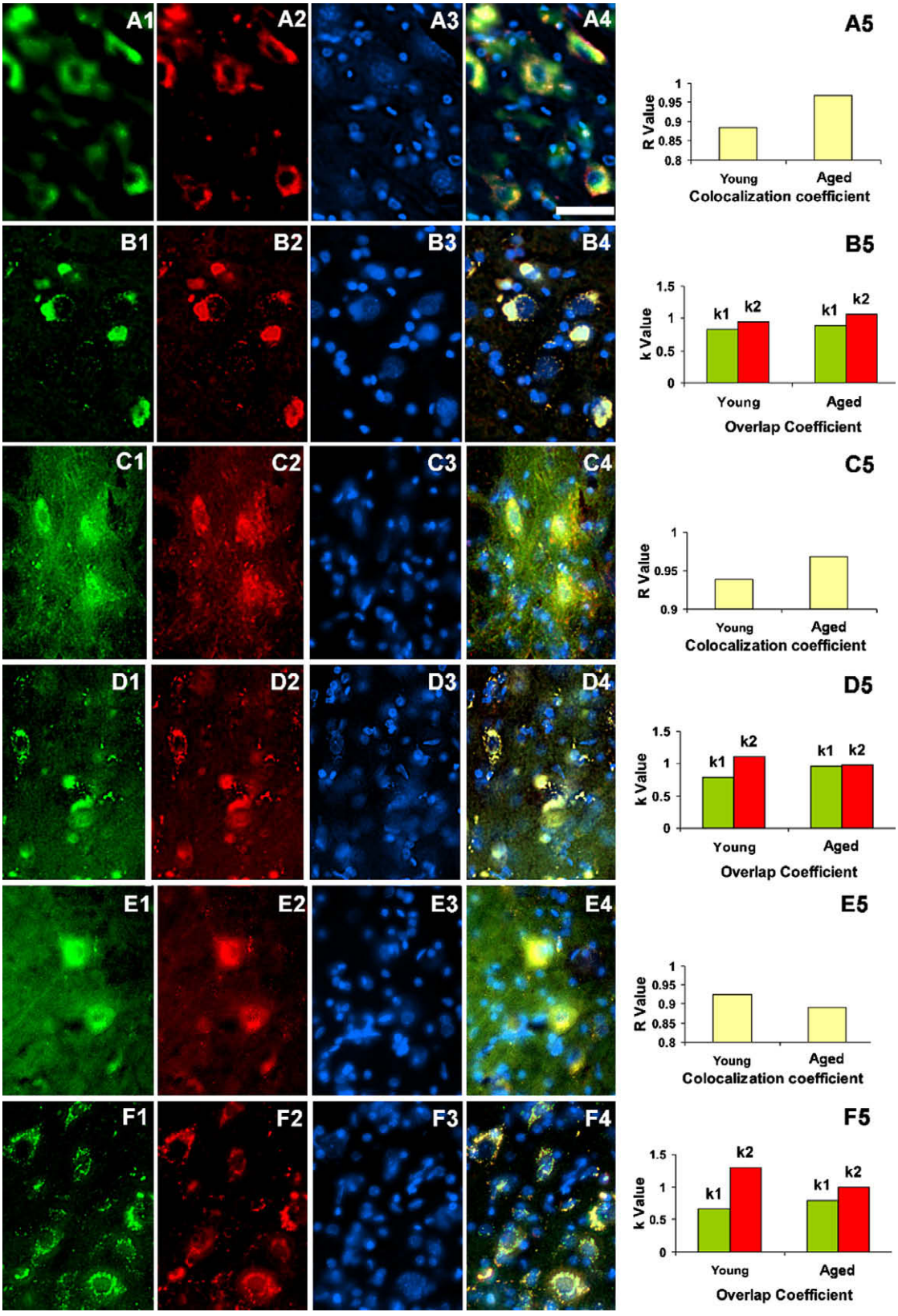

Fig. 5. Immunofluorescence of spinal cord segments of young and aged rats against total PTEN and pPTEN. Rows A–B, C–D and E, F correspond to samples of C5, T8 and L3 segments, respectively, of young (A, C, E) and aged (B, D, F) rats. Column 1 (green) corresponds to the labeling using an anti-PTEN coupled to Alexa 488. Column 2 (red) corresponds to the labeling using an anti-pPTEN coupled to Alexa 555. Column 3 (blue) is the labeling using DAPI. Column 4 is the merge of the three stains. Column 5 shows the colocalization analysis of the analyzed samples (A5–B5 for C5, C5–D5 for T8 and E5–F5 for L3). The colocalization coefficient *R* value was always greater than 85% indicating a significant colocalization of both proteins. The overlap coefficient k2 (pPTEN) was always greater than the corresponding k1 (PTEN) being significant for T8 and L3 in young animals. In all cases, k1 value increased with age. The opposite was true for k2 except for C5. Bar = 50 μm. (For interpretation of the references to color in this figure legend, the reader is referred to the web version of this article.)

small neurons did not statistically vary throughout the laminas ($P = 0.388$) (Fig. 6). The area of medium sized neurons of each lamina of aged rats was always greater than those of young animals (except for Lm-VI) being the difference significant ($P = 0.038$). As for the mean area of large size neurons, cells from aged animals were always larger than young counterparts except for Lm-I and Lm-VII ($P = 0.006$), being Lm-VII and Lm-IX motoneurons where the differences were more remarkable.

For C5 segment, in general, the area of medium sized neurons of each lamina was similar in young and aged animals or larger in young animals. On the contrary, the mean area of large neurons was similar in both age groups or larger in aged animals (data not shown). Moreover, differences in size were statistically significant for large neurons present at Lm-VI and Lm-IX. Considering the shape of the cells, small and medium sized neurons were in general, more elongated in aged animals while large sized cells were more rounded in this group.

4. Discussion

In mice lacking the PTEN gene ($PTEN^{loxP/loxP}$; GFAP-cre mice) the size of the brain and cerebellum becomes progressively larger with time in comparison to normal young animals (Kwon et al., 2006). Histologically, cre mice showed a disarray of Purkinje cells, cell atrophy, reduction of the arborization of dendrites and failure of dendrites to extend completely through the enlarged molecular layer to reach the pial surface (Yue et al., 2005). Moreover, the size of the dentate gyrus granule cells also increased progressively with age. Those cells that maintained PTEN expression in PTEN deficient mice were normal, but those lacking PTEN protein were significantly larger, suggesting that modification in cell size is a direct effect of the absence of PTEN rather than an alteration of the microenvironment. In our study, most of the large sized neurons analyzed in aged rats were larger than their counterparts in young rats. In particular, we have observed a significant increase in the size of motorneurons of the Lamina IX and neurons of Lm-VI. In addition, a decrease in the antagonistic effect of PTEN on the phosphoinositide 3-kinase (PI3K)/pAKT pathway specifically involved in cell growth (Liu et al., 2005) may be postulated. Indeed, most motorneurons from aged rats showed a reduction in the intensity of PTEN expression and even a complete lack of immunoreactivity to that protein was detected in some motoneurons in aged animals.

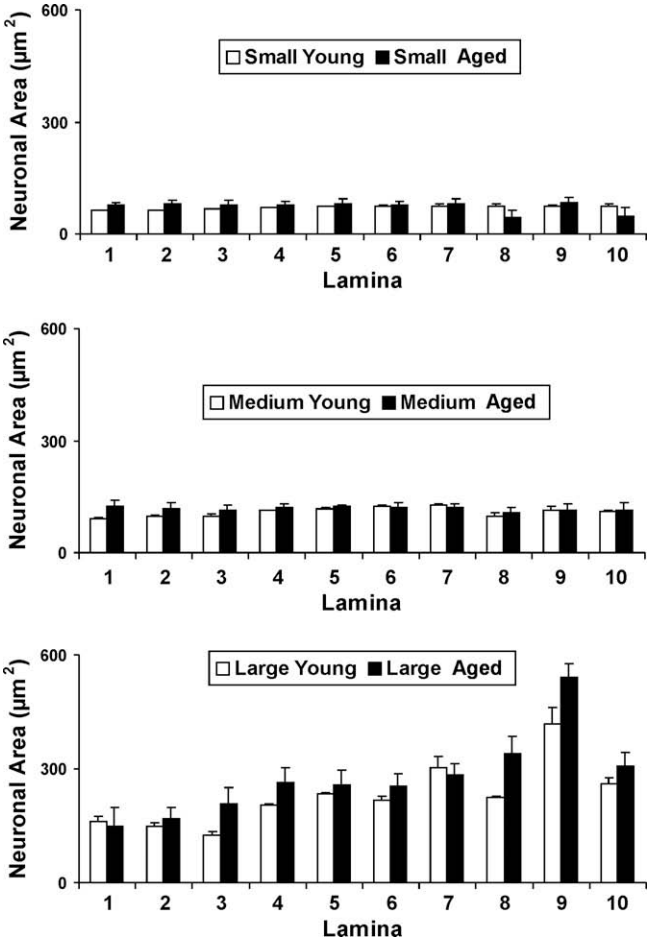

Fig. 6. Area of small, medium and large neuronal cells of young and aged rats. Morphometric analysis revealed that small neurons of both groups were statistically similar ($P = 0.388$). On the other hand, medium and large sized neurons of aged rats were statistically larger ($P = 0.038$ and $P = 0.006$, respectively) in comparison with their young counterparts.

Akt is a serine/threonine kinase and a downstream target in the pathway of the PI3K and is activated by the association of phosphorylated phosphoinositide (PI) generated in reactions catalyzed by PI3K. For complete activation, Akt must be phosphorylated. Akt was shown to have a key role in mechanisms of neuronal survival in the spinal cord. For example, motoneuron survival against excitotoxic injury is regulated by angiogenin in an Akt mediated process (Kieran et al., 2008). Estrogen is also able to regulate neuronal survival following spinal cord injury through the PI3K/Akt pathway (Yune et al., 2008). Furthermore, it has been recently demonstrated that Akt is phosphorylated after spinal cord injury, suggesting a role for this kinase in the response of the spinal cord to damage (Shi et al., 2009).

Akt activity is negatively regulated by molecules that antagonize PI3K, such as PTEN, which control the basal levels of $pAkt^{Ser473}$ and $pAkt^{Thr308}$ (Otaegi et al., 2006). As we have observed in the present study, higher levels of PTEN in the spinal cord of young vs. aged animals were paralleled by low levels of pAkt, suggesting that modifications in the PTEN–PI3K–pAkt pathway may be involved in the changes of neuronal size with aging (Kwon et al., 2001). In addition, considering the neuroprotective role of Akt activation, the increased phosphorylation of Akt in aged rats may also represent a compensatory mechanism against age-related deterioration. A previous study has detected an increase in total Akt immunoreactive cells in the CA1 region of the hippocampus of mice (Eto et al., 2008). It has been proposed that the increase in total levels of Akt may protect against the neuronal dysfunction caused by the activation of calcineurin signaling pathway during the aging processes (Eto et al., 2008). The mechanisms involved in the regulation of Akt levels in the aged brain are unknown. In contrast to the increase of Akt reported in the aged mouse hippocampus, our findings indicate that in the rat spinal cord, total Akt is significantly decreased while Akt phosphorylation is increased with aging. Several factors, including species, sex and regional differences, may explain the different modification of Akt with aging in the rodent hippocampus and the spinal cord. Unfortunately it is unknown whether Akt phosphorylation is affected by aging in the CA1 region of mice. However, it is conceivable that neuroprotective Akt signaling is enhanced in both the CA1 region and the spinal cord, although by different mechanisms: i.e., by an increased Akt expression in the hippocampus and by an increased Akt phosphorylation in the spinal cord.

According to Liu et al. (2005) PTEN is expressed both in the cytoplasm and in the nucleus of normal cells, with a preferential nuclear localization in differentiated or resting cells. Nuclear localization of PTEN is required for the survival of differentiating neuronal cells (Liu et al., 2005). PTEN is biologically functional in the nucleus and mediates growth suppression via signaling mecha-

nisms that differ from those in cytoplasm (Liu et al., 2005). In our study, PTEN was observed both in the cytoplasm and in the cell nucleus of young as well as aged rats. However, the predominant localization at both ages was cytoplasmic. The possible function of PTEN in the neuronal cytoplasm is unknown.

Colocalization was calculated based on the overlap coefficient according to Manders (Zinchuk and Zinchuk, 2006). This coefficient indicates the actual overlap of the fluorescent signals. It represents the true degree of colocalization. This coefficient is insensitive to the limitations of typical fluorescence imaging, such as efficiency of hybridization, sample photobleaching and camera quantum efficiency. On the other hand, the overlap coefficients k1 and k2 were used to determine the contribution of each antigen to the areas with colocalization (Zinchuk and Zinchuk, 2006). This index can help in the understanding of the variations in protein expression. In our experiments a high pPTEN (k2) and low PTEN (k1) was observed in some young spinal cord segments. Although the ratio k2:k1 was not inverted in aged animals, the amount of pPTEN decreased with age. If pPTEN is the inactive form of the PTEN (Odriozola et al., 2007; Vazquez et al., 2001), this age change may represent a mechanism to maintain PTEN activity in spite of its overall decrease in expression. Furthermore our findings are consistent with the hypothesis that Akt regulation in the aged spinal cord is achieved by a modification in PTEN expression rather than by changes in PTEN activity.

In summary, this is to our knowledge, the first study documenting that in the spinal cord of aging rats the expression of PTEN falls and the phosphorylation of Akt increases and that these changes are paralleled by an increase in large neurons (mainly motoneurons) size in the same region. Although these results are descriptive and admittedly do not establish cause–effect relationships, they nonetheless are consistent with the hypothesis that the reported modifications in PTEN and Akt may underlie the increase in spinal cord neuron size observed in aged rats.

Acknowledgments

This work was supported by the FCT (Fundaçao para a Ciencia e Tecnologia) Ph.D. scholarship SFRH/19304/2004/R30Y to MARdeA, Grant PICT 2006-583 from the National Agency for the Promotion of Science and Technology (ANPCyT) to ELP, Ministerio de Ciencia e Innovación, Spain (BFU2008-02950-C03-01) to LMGS, NIH Grant R01AG029798-2 from the National Institute on Aging (NIA) and the Fogarty International Center (FIC), NIH to RGG and ELP and "Luís Santaló" Exchange Program for Fostering Scientific Cooperation sponsored by CSIC-CONICET to LMGS, RGG and ELP. Our gratitude to RJC Cantet for his invaluable help in the statistical analysis. RGG and ELP are Research Career scientists of the Argentine Research Council (CONICET).

References

Agnati, L.F., Fuxe, K., Torvinen, M., Genedani, S., Franco, R., Watson, S., Nussdorfer, G.G., Leo, G., Guidolin, D., 2005. New methods to evaluate colocalization of fluorophores in immunocytochemical preparations as exemplified by a study on A2A and D2 receptors in Chinese hamster ovary cells. J. Histochem. Cytochem. 53, 941–953.

Backman, S.A., Stambolic, V., Suzuki, A., Haight, J., Elia, A., Pretorius, J., Tsao, M.S., Shannon, P., Bolon, B., Ivy, G.O., Mak, T.W., 2001. Deletion of PTEN in mouse brain causes seizures, ataxia and defects in soma size resembling Lhermitte-Duclos disease. Nat. Genet. 29, 396–403.

Eto, R., Abe, M., Hayakawa, N., Kato, H., Araki, T., 2008. Age-related changes of calcineurin and Akt1/protein kinase B alpha (Akt1/PKBalpha) immunoreactivity in the mouse hippocampal CA1 sector: an immunohistochemical study. Metab. Brain Dis. 23, 399–409.

Fraser, M.M., Zhu, X., Kwon, C.H., Uhlmann, E.J., Gutmann, D.H., Baker, S.J., 2004. PTEN loss causes hypertrophy and increased proliferation of astrocytes in vivo. Cancer Res. 64, 7773–7779.

Fontana, P.A., Barbeito, C.G., Goya, R.G., Gimeno, E.J., Portiansky, E.L., 2009. Impact of very old age on the expression of cervical spinal cord cell markers in rats. J. Chem. Neuroanat. 37, 98–104.

Groszer, M., Erickson, R., Scripture-Adams, D.D., Lesche, R., Trumpp, A., Zack, J.A., Kornblum, H.I., Liu, X., Wu, H., 2001. Negative regulation of neural stem/progenitor cell proliferation by the Pten tumor suppressor gene in vivo. Science 294, 2186–2189.

Kieran, D., Sebastia, J., Greenway, M.J., King, M.A., Connaughton, D., Concannon, C.G., Fenner, B., Hardiman, O., Prehn, J.H., 2008. Control of motoneuron survival by angiogenin. J. Neurosci. 28, 14056–14061.

Kwon, C.H., Luikart, B.W., Powell, C.M., Zhou, J., Matheny, S.A., Zhang, W., Li, Y., Baker, S.J., Parada, L.F., 2006. PTEN regulates neuronal arborization and social interaction in mice. Neuron 50, 343–345.

Kwon, C.H., Zhu, X., Zhang, J., Knoop, L.L., Tharp, R., Smeyne, R.J., Eberhart, C.G., Burger, P.C., Baker, S.J., 2001. PTEN regulates neuronal soma size: a mouse model of Lhermitte-Duclos disease. Nat. Genet. 29, 404–411.

Littell, R.C., Henry, P.R., Ammerman, C.B., 1998. Statistical analysis of repeated measures data using SAS procedures. J. Anim. Sci. 76, 1216–1231.

Liu, J.L., Sheng, X., Hortobagyi, Z.K., Mao, Z., Gallick, G.E., Yung, W.K., 2005. Nuclear PTEN-mediated growth suppression is independent of Akt down-regulation. Mol. Cell. Biol. 25, 6211–6224.

Lozza, F.A., Chinchilla, L.A., Barbeito, C.G., Goya, R.G., Gimeno, E.J., Portiansky, E.L., 2009. Changes in carbohydrate expression in the cervical spinal cord of rats during aging. Neuropathology 29, 258–262.

Odriozola, L., Singh, G., Hoang, T., Chan, A.M., 2007. Regulation of PTEN activity by its carboxyl-terminal autoinhibitory domain. J. Biol. Chem. 282, 23306–23315.

Otaegi, G., Yusta-Boyo, M.J., Vergaño-Vera, E., Méndez-Gómez, H.R., Carrera, A.C., Abad, J.L., González, M., de la Rosa, E.J., Vicario-Abejón, C., de Pablo, F., 2006. Modulation of the PI 3-kinase-Akt signalling pathway by IGF-I and PTEN regulates the differentiation of neural stem/precursor cells. J. Cell Sci. 119, 2739–2748.

Portiansky, E.L., Barbeito, C.G., Gimeno, E.J., Zuccolilli, G.O., Goya, R.G., 2006. Loss of NeuN immunoreactivity in rat spinal cord neurons during aging. Exp. Neurol. 202, 519–521.

Rexed, B., 1952. The cytoarchitectonic organization of the spinal cord in the cat. J. Comp. Neurol. 96, 415–496.

Ross, A.H., Lachyankar, M.B., Recht, L.D., 2001. PTEN: a newly identified regulator of neuronal differentiation. Neuroscientist 7, 278–281.

Shi, T.J., Huang, P., Mulder, J., Ceccatelli, S., Hökfelt, T., 2009. Expression of p-Akt in sensory neurons and spinal cord after peripheral nerve injury. Neurosignals 17, 203–212.

Schüz, A., Palm, G., 1989. Density of neurons and synapses in the cerebral cortex of the mouse. J. Comp. Neurol. 286, 442–455.

Stiles, B., Groszer, M., Wang, S., Jiao, J., Wu, H., 2004. PTEN less means more. Dev. Biol. 273, 175–184.

van Diepen, M.T., Eickholt, B.J., 2008. Function of PTEN during the formation and maintenance of neuronal circuits in the brain. Dev. Neurosci. 30, 59–64.

Vazquez, F., Grossman, S.R., Takahashi, Y., Rokas, M.V., Nakamura, N., Sellers, N.R., 2001. Phosphorylation of the PTEN tail acts as an inhibitory switch by preventing its recruitment into a protein complex. J. Biol. Chem. 276, 48627–48630.

Yue, Q., Groszer, M., Gil, J.S., Berk, A.J., Messing, A., Wu, H., Liu, X., 2005. PTEN deletion in Bergmann glia leads to premature differentiation and affects laminar organization. Development 132, 3281–3291.

Yune, T.Y., Park, H.G., Lee, J.Y., Oh, T.H., 2008. Estrogen-induced Bcl-2 expression after spinal cord injury is mediated through phosphoinositide-3-kinase/Akt-dependent CREB activation. J. Neurotrauma 25, 1121–1131.

Zinchuk, O., Zinchuk, V., 2006. Dynamics of cellular responses studied by quantitative colocalization analysis. Am. Microsc. Anal. Life Sci. Suppl., S5–S7.